STRUCTURAL VIBRATION AS A NOISE SOURCE ON VIBRATING SCREENS

David S. Yantek
National Institute for Occupational Safety and Health
Pittsburgh, PA, USA

Hugo R. Camargo
National Institute for Occupational Safety and Health
Pittsburgh, PA, USA

ABSTRACT

A-weighted sound levels around vibrating screens in coal preparation plants often exceed 90 dB(A). The National Institute for Occupational Safety and Health (NIOSH) is actively developing noise controls to reduce noise generated by horizontal vibrating screens. A 121-microphone, 3.5-meter-diameter array was used to perform beamforming to determine locations of significant noise radiation on the screen. Below about 1 kHz, the screen body was found to be the most significant noise source. The beamforming contour maps showed several key locations on the sides of the screen and the feedbox are the most significant contributors. Operating deflection shape (ODS) analysis was used to examine the screen behavior under actual operating conditions. This information is helpful in determining how to modify the screen body to reduce the noise radiated by the screen below 1 kHz. The analysis showed modal vibration patterns on the sides and feed box were the main contributors to noise. The results show several areas on the screen sides and feedbox that can be modified to reduce noise.

INTRODUCTION

In 1996, NIOSH published the National Occupational Research Agenda (NORA), which identified hearing loss as the most common job-related disease in the United States [1]. Approximately 30 million workers are exposed to hazardous sound levels alone or to hazardous sound levels in conjunction with ototoxic agents [2]. Despite more than 30 years of noise regulation in the mining industry, mine workers develop hearing loss at a significantly higher rate compared to the non-noise exposed population. An analysis of audiograms conducted by NIOSH in 1996 shows that by the age of 50, nearly 90% of coal miners had a hearing impairment [3]. In contrast, only 10% of those who are not exposed to occupational noise experienced a hearing loss by the same age.

The Mine Safety and Health Administration (MSHA) modified its rules regarding noise exposure in 1999 in an effort to reduce the occurrence of noise-induced hearing loss [4].

Rather than relying solely on hearing protection devices, MSHA's new rule requires mine operators to use all feasible engineering and/or administrative controls to reduce the noise exposures of overexposed miners'. However, for many machines, such as vibrating screens, noise controls that reduce the operator's noise exposure below the MSHA Permissible Exposure Level (PEL) are not currently available.

In 2000, there were 212 preparation plants in operation in the US and 129 of these plants were located in three states: Kentucky, Pennsylvania, and West Virginia [5]. NIOSH studies have shown that workers who spend a significant portion of their shift working in a coal preparation plant can experience noise exposures which exceed the MSHA PEL for noise. NIOSH data show that 20 out of 46 coal preparation plant workers had noise exposures that exceeded the MSHA PEL noise dose [6]. MSHA PEL noise doses up to 220% have been recorded for preparation plant workers in jobs with titles such as stationary equipment operator, froth cell operator, plant operator, plant controls man, third floor operator, wet plant attendant, sump floor operator, plant backup, and plant mechanic. These job classifications require the worker to spend a significant portion of a shift in the plant while working around slurry pumps, dryers, centrifuges, and vibrating screens.

A horizontal vibrating screen (see Figure 1) is a large machine used to process clean coal that has been separated from refuse materials using a water-magnetite mixture. This magnetite is recovered because the magnetite lowers the heating value of coal and it can be re-used in the processing plant. The screen body has four sides made of steel plates with a bottom screening surface made of steel wire welded to a frame with small gaps between the wires. The body of the screen is supported on a steel coil spring suspension. One or more vibration mechanisms are mounted to a steel beam that spans the width of the screen. These vibration mechanisms, which use rotating eccentric shafts to generate vibration, are belt-driven using an electric motor. The screen is designed such that it vibrates on roughly a 45-degree angle. Coal flows into

the feed end of the screen from a delivery chute. As the screen the material moves along the deck and under a water spray that rinses the magnetite from the coal. The liquid and fine coal particles pass through the gaps in the screening deck as the material flows toward the discharge end of the screen. Finally, the rinsed coal falls off the discharge end of the chute to continue with further processing.
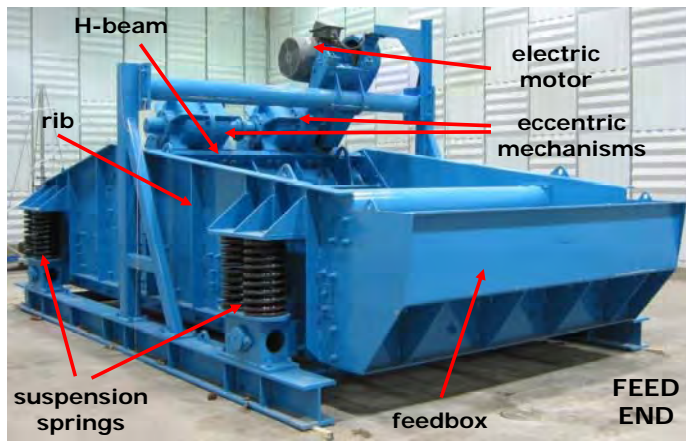
(a)
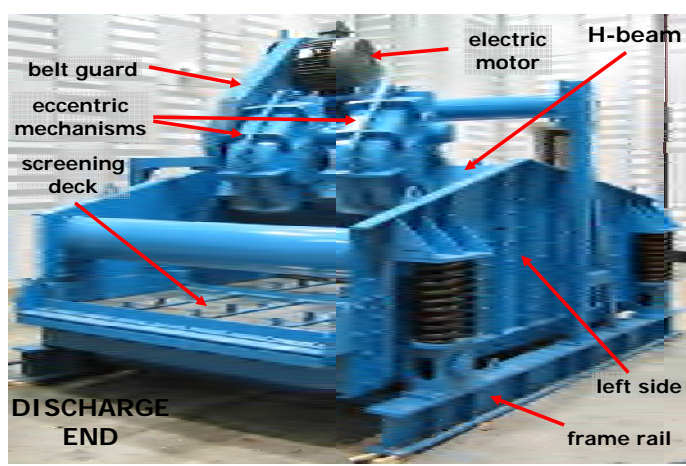
(b)

Figure 1. A horizontal vibrating screen as viewed from (a) feed end and (b) discharge end.

Since they are used to size, separate, and dewater both coal and refuse (rock) of various sizes, screens may be located on many floors within a preparation plant. The number of screens in a processing plant can range from a single screen to more than a dozen. Consequently, preparation plant workers can be exposed to high sound levels generated by screens multiple times during a shift as they move and work throughout the plant. Vibrating screens are a major noise problem in most coal preparation plants because screens are used extensively in plants, are usually located in high traffic areas, and can generate high noise levels [7]. The objective of this paper is to examine the noise radiated by horizontal vibrating screens below 1 kHz.

vibrates,

NIOSH performed sound level measurements near a group of eight horizontal vibrating screens used to process clean coal [8]. These measurements indicated that the sound levels ranged from 94 to 98 dB(A) with the plant processing coal. With the coal flow turned off and the screen vibration mechanisms turned on, the sound levels ranged from 89 to 97 dB(A). The sound levels decreased significantly with increasing distance from the screens, indicating that the screens dominate the overall A-weighted sound level in this area of the preparation plant. In order to reduce the potential for overexposing preparation plant workers to noise, noise controls must be developed to address dominant noise sources on the screen.

The sound power level of a screen was measured in the NIOSH reverberation chamber. The data show that the one-third-octave-band sound power levels below 1 kHz account for roughly 80% of the overall A-weighted sound power level. NIOSH applied the beamforming technique using a 42-microphone, 1.9-meter-diamteter array to identify noise sources on a vibrating screen [9]. Data were collected with the array positioned to the front, rear, and sides of the machine with the screen in the NIOSH hemi-anechoic chamber. The results showed that the vibration mechanism housings, belt guard, and steel coil springs are the dominant noise sources from 1 kHz through 3.15 kHz. The 42-microphone array was too small to examine noise radiated below 1 kHz.

The noise radiated by the screen at frequencies below 1 kHz was examined because this frequency range accounts for about 80% of the overall A-weighted sound power level. The dominant noise sources at these frequencies must be addressed to reduce the radiated noise. Since the screen is relatively large, sound intensity and near field acoustic holography would require numerous measurements to examine the sources from all sides of the screen. Beamforming enables researchers to perform relatively few measurements to examine noise radiation. However, a large array must be used to achieve sufficient spatial resolution. Operating deflection shape (ODS) analysis was used to examine the vibration patterns on the screen. This information is essential to understand how to modify the screen to reduce noise. In addition, the sound power level radiated by the sides and feed box was estimated using the ODS data.

NOMENCLATURE

$[X]$ Response matrix

$[H]$ Frequency response function matrix

$[F]$ Force matrix

L_W sound power level

$\langle v \rangle_{s,t}^2$ surface averaged mean-squared velocity

S surface area

σ   radiation efficiency

BEAMFORMING MEASUREMENTS AND RESULTS

NIOSH contracted Acoustical and Vibration Engineering Consultants (AVEC) to perform beamforming measurements using their 121-microphone, 3.5-meter-diameter array. The vibrating screen was positioned in the center of the NIOSH hemi-anechoic chamber. The chamber dimensions are approximately 16.7 meters long, 10.1 meters wide, and 7.0 meters high. AVEC's phased array is an 11-arm star array with a proprietary microphone arrangement. The array was mounted to a movable truss to position the array for measurements from each screen surface (see Fig. 2). It was mounted in two configurations: vertical (microphone plane perpendicular to the floor) and horizontal (microphone plane parallel to the floor). With the array in the horizontal configuration, data were collected at three positions above the screen. Data was also collected from each side of the machine with the array in the vertical configuration.

A 128-channel acquisition system with proprietary signal conditioning and anti-aliasing filtering was used to collect the microphone data. All microphone signals were sampled simultaneously using a sampling frequency of 51.2 kHz. For each measurement, 16 seconds of continuous data were collected. This data was post-processed using AVEC beamforming analysis software. The results were examined in one-third-octave bands. Contour maps were computed for each array position using conventional beamforming with diagonal removal [10]. Multiple source plane, or calculation plane, distances were used to process the data for each measurement. This provides the ability to examine noise sources at different depths relative to the array. Due to space limitations, only the most significant results will be discussed.

Prior to examining screen data, a test was conducted with a loudspeaker to examine the spatial resolution. The researchers confirmed the spatial resolution of the array was adequate down to 250 Hz. For the 250 Hz one-third-octave band, the contour maps appear to indicate the screen sides were the most significant source (see Fig. 3). Most of the noise radiation appears to occur from approximately the center of the screen side.

(a)

(b)

Figure 2. AVEC array mounted to a truss in the (a) vertical configuration and (b) horizontal configuration.
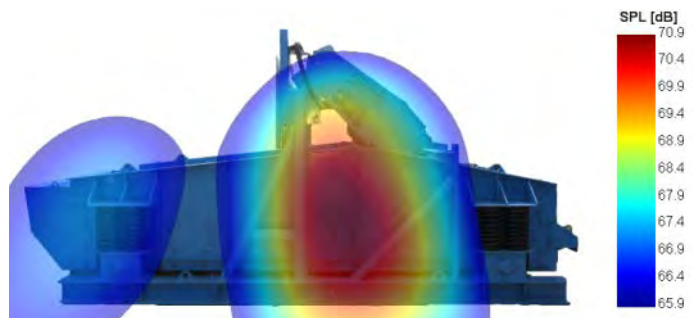

Figure 3. Beamforming results for the rt. side for the 250 Hz 1/3-OB.

Figure 4 shows the contour maps with the array positioned above the discharge end of the screen and with the array centered above the screen for the 315 Hz one-third-octave band. The images in Fig. 4 appear to indicate several locations of high noise radiation along the screen sides and from the feed box. Multiple ribs are positioned along the screen sides to increase the stiffness of the plates that make up the sides. The spacing between the ribs is non-uniform. The area of high noise radiation near the discharge end of the screen (see Fig. 4a) corresponds to the location just in front of the large H-beam that connects the screen sides. The area of high noise radiation on the screen sides towards the feed end of the machine (see Fig. 4b) corresponds to locations just in front of a large tube that connects the screen sides. It is interesting to note that the locations near the feed and discharge ends of the screen that have the highest noise radiation are in areas with the largest spans between the ribs. Figure 4b clearly indicates the back and/or the bottom of the feed box are also significant contributors to noise radiated in this band.
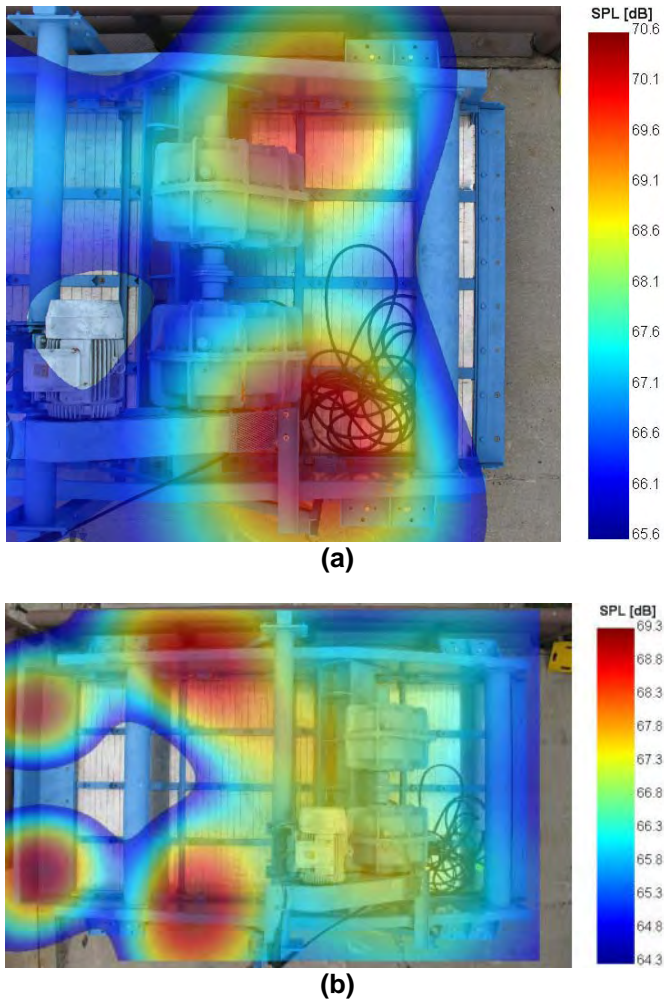
For the 400 Hz one-third-octave band, the screen sides appear to be the most significant noise sources. Figure 5 shows resulting contour map with the array positioned at the discharge end (a) and with the array to the right side (b). The calculation planes for these images correspond to the plane of the electric motor and the screen side, respectively. The image from the discharge end of the screen indicates two sources that seem to be along the sides of the screen. The contour for the screen side clearly shows most of the noise is radiated from the sides. The area of highest radiation matches the area between two ribs just below where the H-beam connects to the screen sides.

(a)

(b)

Figure 4: Beamforming results for the 315 Hz 1/3-OB with array (a) over discharge end and (b) over center.
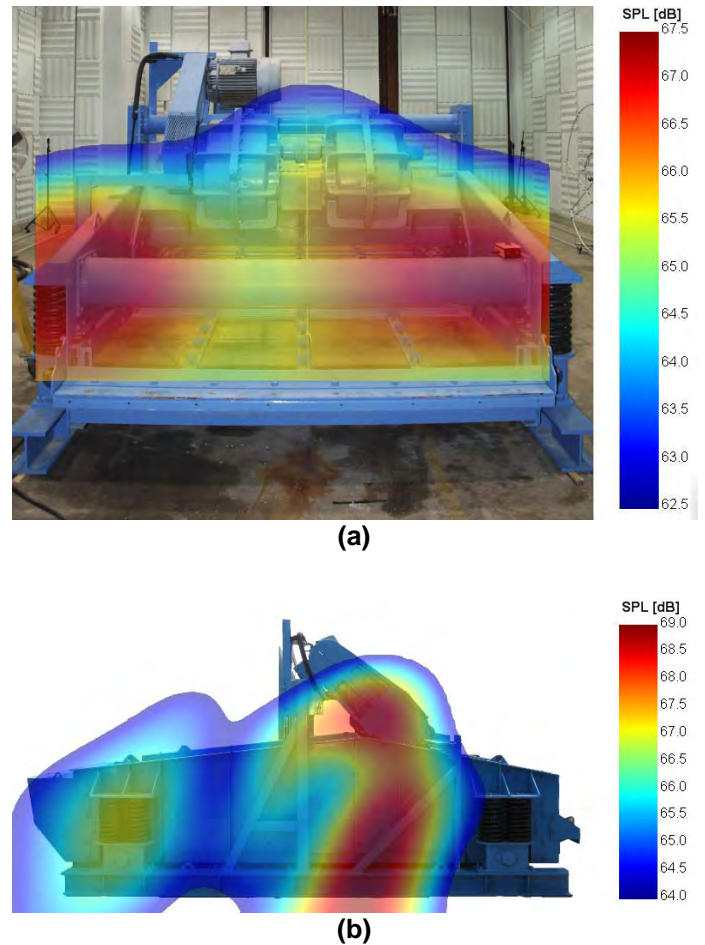

(a)

(b)

Figure 5: Beamforming results for the 400 Hz 1/3-OB with (a) array at discharge end and (b) array to rt. side.

Figure 6 shows the contour map for the right side of the screen with the calculation plane at the screen side. Once again, the highest radiation appears to correspond to the area between two ribs and below the H-beam attachment point. A secondary source appears to match the area just above the screen suspension brackets.
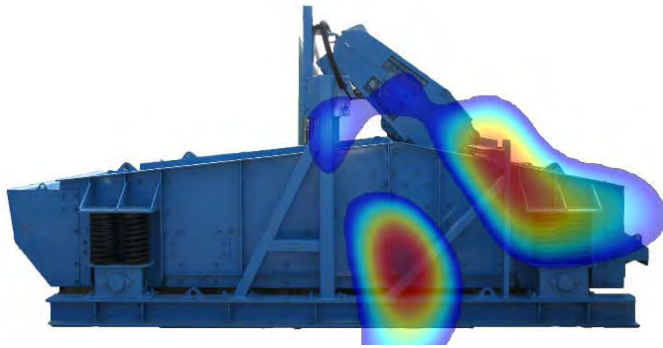
Figure 6. Beamforming results for the 500 Hz 1/3-OB for the rt. side with calculation plane at screen side.

Figure 7 shows the beamforming image for the right side of the screen with the calculation plane at the screen side. The image shows the most significant source is at a location between two stiffeners that is just behind the H-beam attachment location. A secondary source is shown near the top of this panel. The image also shows either the belt guard or the right vibration mechanism housing is also a significant source.
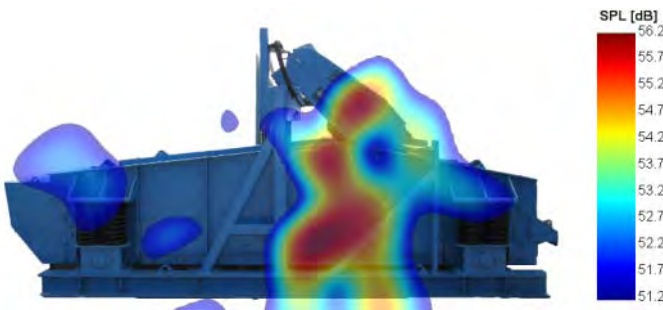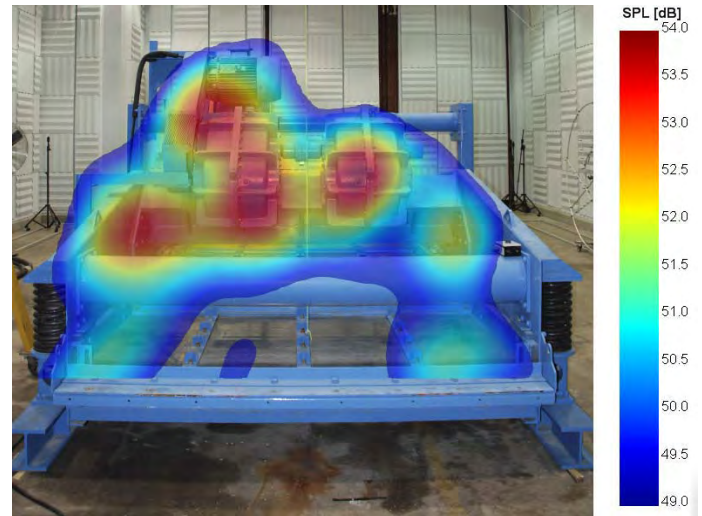

Figure 7. Beamforming results for the 630 Hz 1/3-OB for the rt. side with calculation plane at screen side.

The contour map for the 800 Hz one-third-octave band with the calculation plane at the eccentric shaft location is shown in Fig. 8a. Several sources appear to be significant for this band. Both the left and right vibration mechanism housings are shown to be sources. In addition, the area between the belt guard and the right vibration mechanism housing appears to be a source of high noise radiation. Finally, two areas along the screen sides appear to be significant. The image for the right side confirms the location of the sources along the screen side (see Fig. 8b). Once again this location coincides with a location between two stiffeners that is just below the H-beam attachment point.

The results for the 1 kHz one-third-octave band are shown in Fig. 9 with the source plane set to the eccentric motor location. The image from the discharge end indicates the area near the top of the right vibration mechanism and the electric motor is the most significant contributor to noise in this band.

The image from above the screen shows the electric motor is the most significant source for this band.


(a)
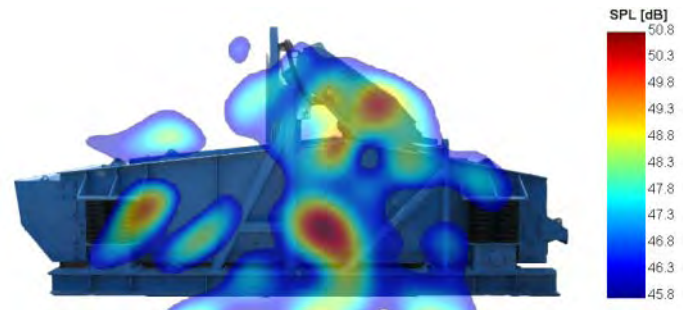
(b)

Figure 8. Beamforming results for the 800 Hz 1/3-OB with array (a) at feed end and (b) to rt side.

The beamforming results point to the screen sides and feed box as dominant noise sources for each one-third-octave band in the 250 Hz through 800 Hz bands whereas the electric motor appears to be the most significant source for the 1 kHz band. It should be noted that beamforming has a limited range in terms of identifying noise sources. In most cases, only the top 6 to 15 dB of noise sources can be identified with this technique. Since structural vibration at lower frequencies is generally of a global nature, further analysis was needed to understand the screen's dynamic behavior for the bands below 800 Hz. Therefore, ODS data collection and analysis was performed.
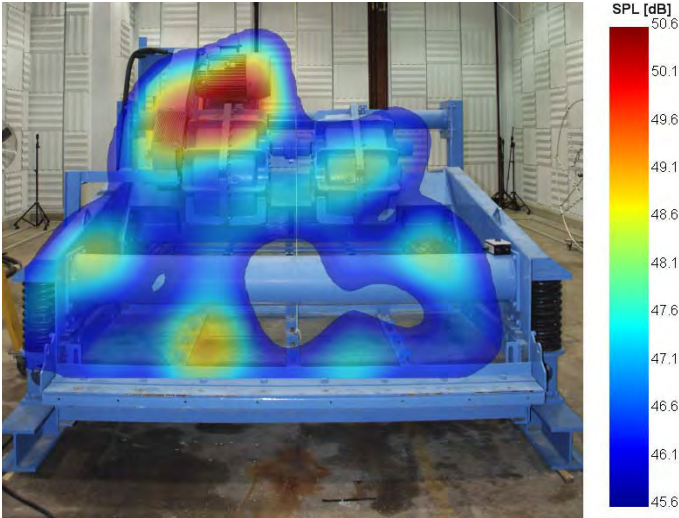
(a)
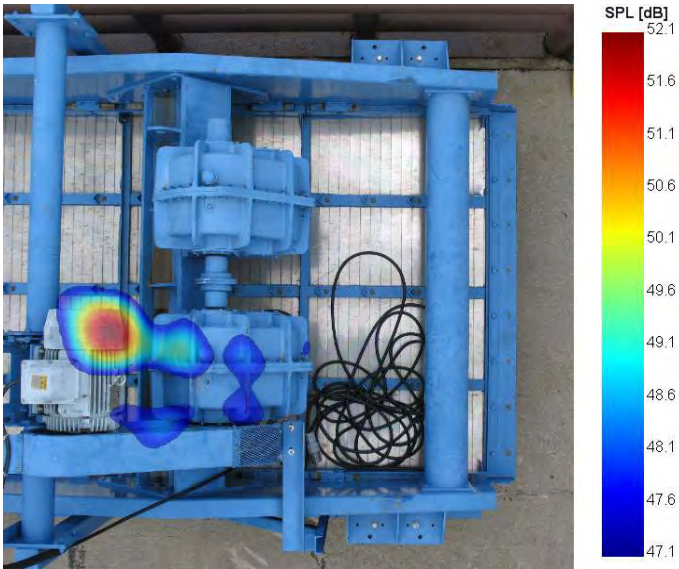
(b)

Figure 9. Beamforming results for the 1 kHz 1/3-OB with the array (a) at the discharge end and (b) above the discharge end.

OPERATING DEFLECTION SHAPE TESTING AND ANALYSIS

Structural vibration is complex in nature. All structures exhibit their own dynamic characteristics that depend on the mass, stiffness, and damping of the structure. Structures exhibit resonant frequencies that yield high vibration and noise levels when excited by operating forces. Each resonant frequency has its own characteristic shape referred to as a mode shape. The response of a structure to a vibratory input force is described by

$$[X] = [H][F] \tag{1}$$

where $[X]$ is the displacement at each location, $[H]$ is the transfer function matrix, and $[F]$ is the matrix of applied forces [11]. The transfer function matrix is a function of frequency; hence it is sometimes called the frequency response function (FRF) matrix. The FRF matrix depends on the mass, stiffness, and damping of a structure and it contains all the natural frequency and mode shape information of a structure.

Experimental modal analysis is a technique that is used to extract the natural frequencies and mode shapes of a structure. In the application of this technique, broadband excitation is applied to the structure using either an impact hammer or one or more electromechanical shakers at discrete locations. The applied forces and resulting vibration at numerous locations are measured and FRFs are computed between each force and response location. This data is then curve fit to determine the natural frequencies and mode shapes. This data can be used to examine the dynamic characteristics of a structure and for purposes of benchmarking finite element models, for example.

However, the actual behavior of an object subject to vibration is the result of both the natural frequencies and mode shapes of the structure and the real operating forces. ODS testing is a technique that can be applied to examine this operating behavior. The operating forces do not have to be measured when performing ODS testing. In practice, the vibration at numerous locations is measured on a structure by roving one or more accelerometers around the structure. In addition, one or more reference accelerometers are positioned at fixed locations. For frequency-based ODS testing, the measured autopower spectra at each location is computed along with the cross-spectra between the roving accelerometers and the reference accelerometer(s). The autopower spectra are used to determine the magnitude of the response at each location and the cross-spectra are used to determine the phase relationship between the roving accelerometer(s) and the reference(s). The resulting data can be animated (or plotted) to examine the resulting operating deflection shapes.

To analyze the operating vibration of the screen, ODS measurements were performed (see Fig. 10) using Bruel & Kjaer ODS Consultant software. Uniaxial accelerometers were used to measure operating vibration at over 400 locations. At most of the locations, only the vibration normal to the surface was measured, since this is the most useful in terms of noise radiation. Three reference accelerometers were used. One reference accelerometer was fixed to the left side of the screen near the feed end and one was attached to the right side of the screen near the discharge end. A third reference accelerometer was attached to the H-beam. The data were collected with a bandwidth of 1600 Hz.

6

Figure 10. Researchers roving accelerometers during ODS testing.

Prior to animating the collected ODS data, the sound power level radiated by the screen sides was estimated using:

$$L_W = 10\,log_{10}\langle v\rangle^2_{s,t} + 10\,log_{10} S + \\ 10\,log_{10}\,\sigma + 146 \tag{2}$$

where L_W is the sound power level, $\langle v\rangle^2_{s,t}$ is the surface averaged mean-squared velocity, S is the surface area, and σ is the radiation efficiency. To obtain the surface average velocity, the measured acceleration autopower spectra were integrated in the frequency domain. In the analysis, each portion of the screen was separated into panels between rib stiffeners. The perimeter and thickness of the steel panels were used to determine the radiation efficiency [12].

Figure 11 shows the estimated sound power level from each screen side and the feed box. The figure shows the surfaces have significant contributions to the sound power level in the 100 Hz one-third-octave band through the 800 Hz one-third octave bands. Previous research identified the 200 Hz through 800 Hz frequency range as the dominant frequency range for the measured A-weighted sound power level [9]. Each of the three surfaces has comparable estimates of radiated sound power. In order to significantly reduce the noise in this frequency range, all three screen components must be addressed.
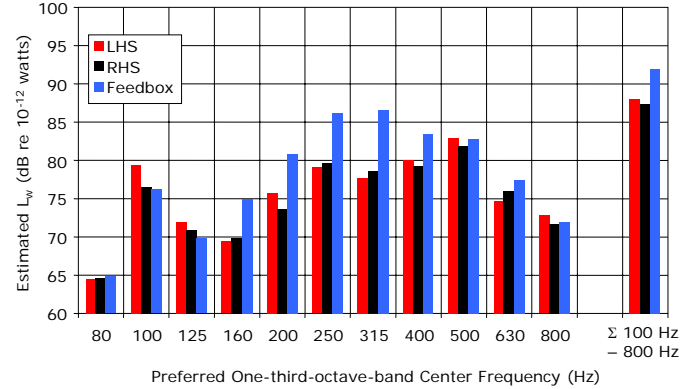

Figure 11. Estimated sound power level radiated by the screen sides and feedbox.

A wire frame model of the screen was made in ME'scope software (see Fig. 12). The collected data were imported into ME'scope. The data were examined for peaks in the acceleration autopower spectra that coincide with frequencies of high noise radiation. The operating deflection shapes were then examined at these frequencies. To be succinct, only selected results will be presented here. For each of these figures, the color indicates the amount of motion at each location.

Two of the operating deflection shapes for peaks that are in the 100 Hz one-third-octave band are shown in Fig. 13. Each shape is dominated by motion along the screen sides. For the shape at 92 Hz, the sixth panel along each side exhibits dominant motion whereas the shape at 107 Hz is dominated by motion at the seventh panel. In each case, the motion of the panel is similar to the first mode of vibration of a plate with fixed boundary conditions.
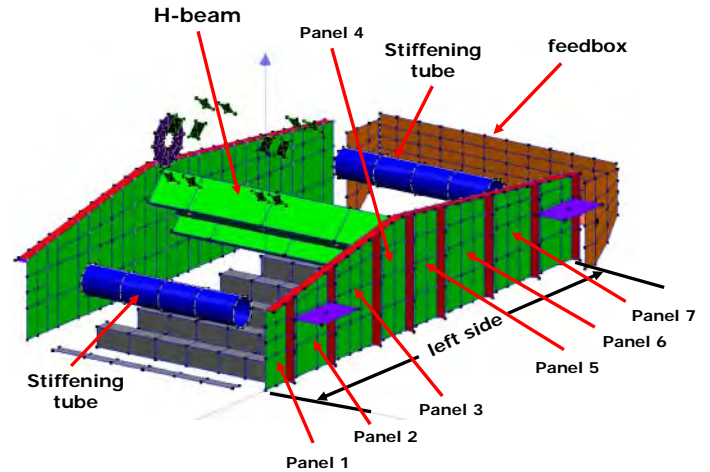

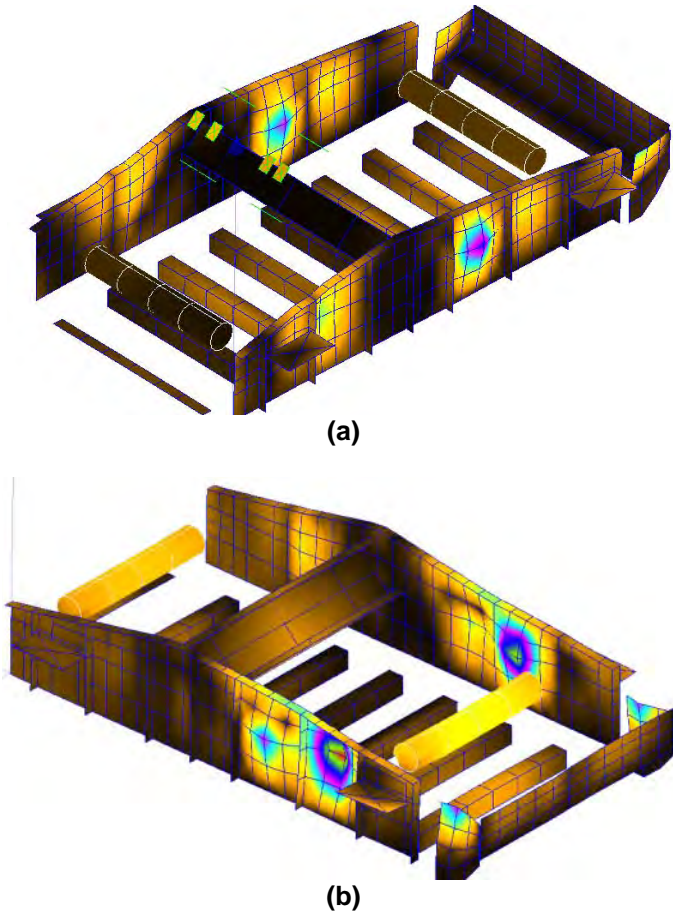**Figure 12. ME'scope wireframe model of the screen.**

(a)

(b)
Figure 13. Operating deflection shapes for (a) 92 Hz and (b) 107 Hz.

(a)

(b)
Figure 14. Operating deflection shapes at (a) 182 Hz and (b) 204 Hz.

Figure 14 shows two operating deflection shapes in the 200 Hz one-third-octave band. The shape at 182 Hz is dominated by bending of the back panel of the feedbox. In addition, the third and sixth panels on the left side and the sixth panel on the right side undergo significant motion. In this case, a nodal line exists between the upper and lower portions of the panels. The shape at 204 Hz shows the feedbox and the third, fifth, sixth, and seventh panels have the dominant motion. The motion at the fifth panel is confined to the bottom portion of the panel. It is interesting to note that the top of the fifth panel is the location where the H-beam connects to the screen sides.
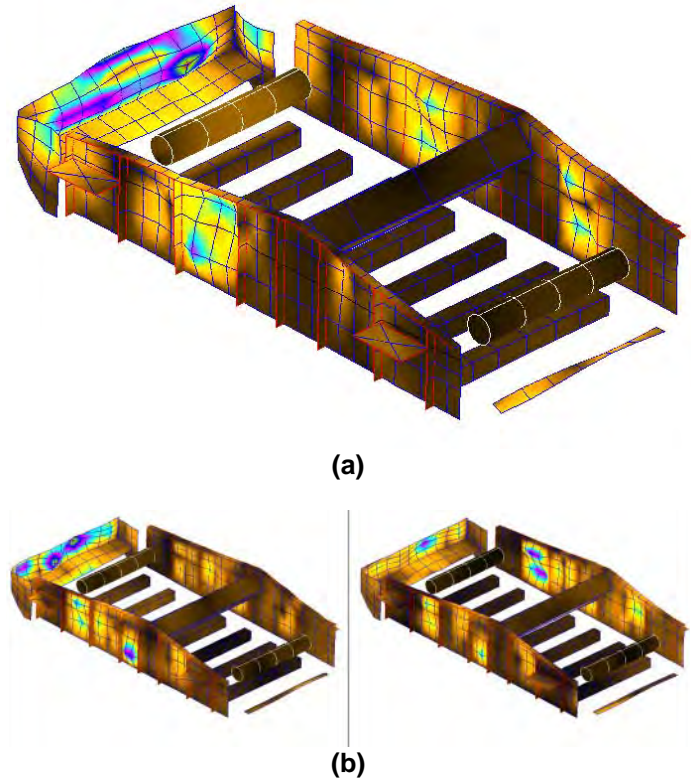
Two of the operating deflection shapes for frequencies in the 250 Hz one-third-octave band are shown in Fig. 15. The motion for the shape at 239 Hz is dominated by motion of the feedbox. The motion on the back of the feedbox shows five regions of high vibration levels. The shape at 253 Hz is dominated by motion at the sixth and seventh panels along the screen sides. In this case, the sixth and seventh panels exhibit vertical nodal lines. The back and inside of the feedbox also exhibit significant motion.
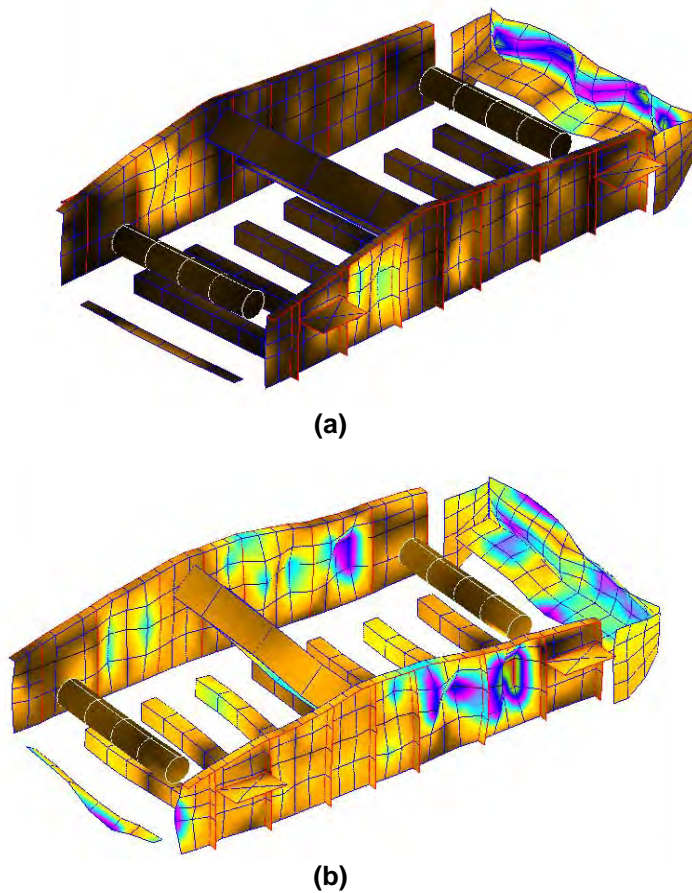
(a)

(b)

Figure 15. Operating deflection shapes for (a) 239 Hz and (b) 253 Hz.

(a)

(b)

Figure 16. Operating deflection shapes for (a) 332 Hz and (b) 337 Hz.

Figure 16 shows two operating deflection shapes for frequencies within the 315 Hz one-third-octave band. Each of these shapes is dominated by motion of the back and sides of the feedbox. Each shape also shows significant motion at the seventh side panel. However, for these shapes, the motion on the screen sides is somewhat more distributed than the other shapes presented here.

After comparing the presented operating deflections shapes, it appears that there are some common areas of significant motion among the shapes. The back of the feedbox exhibits significant motion for all of these shapes except those in the 100 Hz one-third-octave band. In addition, some combination of the third, fifth, sixth, and seventh panels have significant motion for all the presented shapes. Noise controls should focus on these key areas in order to produce the largest reductions in noise with the fewest changes.
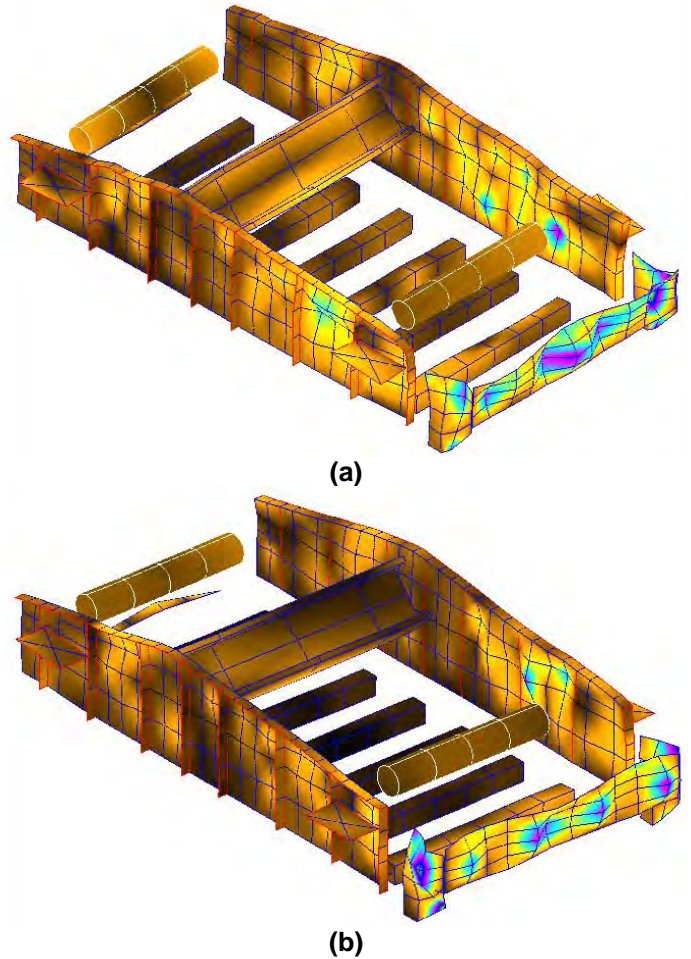
NOISE CONTROLS FOR THE SCREEN BODY

The excitation source for the presented operating deflections shapes is most likely bearing slap within the vibration mechanisms. The bearings for these machines must incorporate clearance within the bearings to reduce heat generation. This clearance probably results in relative motion between the eccentric shafts and the bearing housings of the vibration mechanisms. In effect, this provides a source of broadband excitation to the structure which excites the structural modes of the screen.

In order to reduce the motion on the screen body, some combination of stiffness and damping treatments could be applied. Increasing the plate thickness would increase the stiffness of the structure and slightly increase the resonant frequencies for the structure. This would reduce the amplitude of motion for the presented deflection shapes. However, increasing the plate thickness substantially would require the eccentric force to be increased to maintain the same processing capability. This in turn would require more durable bearings.

Application of constrained layer damping to the screen sides and feedback would reduce the amplitude of motion at the resonant peaks that are excited during operation. This might also make a substantial noise reduction. However, this also may be unacceptable to the screen manufacturer due to the additional weight for the reasons discussed above.

Perhaps the best combination of screen modifications would be to add stiffeners and damping treatments to selected locations based on the operating deflection shapes presented above. For example, rib stiffeners could be added to the panels on the screen sides and feedback where the most significant motion occurs. Stiffeners could be positioned so that each stiffener crosses the areas near the maximum motion for the panel in question. In addition, constrained layer damping treatments could be applied to these areas to reduce motion.

It is important to note that adding rib stiffeners can increase the radiation efficiency of panels due to the increase in the perimeter when a stiffener is added. However, it may be possible to increase the modal stiffness so that the reduction in vibration outweighs the increase in radiation efficiency.

CONCLUSIONS

A 121-microphone phased array was used to perform beamforming measurements on a vibrating screen. The beamforming results indicate the screen sides and feed box are dominant noise sources for the 250 Hz through 800 Hz one-third-octave bands whereas the electric motor appears to be the most significant source for the 1 kHz band. Operating deflection shape analysis showed several key areas are the main locations of high motion for vibration in the 100 Hz, 200 Hz, 250 Hz, and 315 one-third-octave bands. The back and sides of the feedback and the third, fifth, sixth, and seventh panels on the screen sides have significant motion for the presented shapes. Noise controls should target these areas in order to reduce noise generated by the screen.

ACKNOWLEDGMENTS

REFERENCES

[1] National Institute for Occupational Safety and Health, "National Occupational Research Agenda," DHHS (NIOSH) Publication No. 96-115 (1996).

[2] National Institute for Occupational Safety and Health, "Preventing occupational hearing loss – a practical guide," Edited by Franks, J, MR Stephenson, and CJ Merry. DHHS (NIOSH) Publication 96-110, 91p. (1996)

[3] JR Franks, Analysis of Audiograms for a Large Cohort of Noise-Exposed Miners. Unpublished technical report. NIOSH, Cincinnati, OH: (1996)

[4] Department of Labor, Mine Safety and Health Administration, "Health Standards for Occupational Noise Exposure: Final Rule," 30 CFR Part 62. Federal Register (1999).

[5] S. Fiscor and J. Lyles, "Prep Plant Population Reflects Industry," Coal Age, October, pp. 31-38. (2000)

[6] E.R Bauer, Personal communication. DHHS, CDC, NIOSH, PRL, Pittsburgh, PA. (2004).

[7] M.N. Rubin, A.R. Thompson, R.K. Cleworth, and R.F. Olson. Noise Control Techniques for the Design of Coal Preparation Plants (Contract J0100018, Roberts & Schaefer Company and Bolt Beranek and Newman Inc.), BuMines OFR 42-84, 125 pp. (1982).

[8] D. Yantek, P. Jurovcik, and E.R. Bauer. "Noise and Vibration Reduction of a Vibrating Screen," 2005 SME Annual Meeting, preprint 05-71, (Society for Mining, Metallurgy, and Exploration, Inc., Littleton, CO, 2005).

[9] D. Yantek, H. Camargo, and R. Matetic, "Application of a microphone phased array to identify noise sources on a horizontal vibrating screen," Noise-Con 2008.

[10] Thomas Mueller (ed.), Aeroacoustic Measurements, Springer, 2002. ISBN 3-540-41757-5.

[11] P. McHargue and M. Richardson. "Operating Deflection Shapes from Time Versus Frequency Domain Measurements", Presented at the 11th International Modal Analysis Conference, Orlando FL, February 1993.

[12] D.A. Bies and C.H. Hansen, Engineering Noise Control Theory and Practice. Third Edition. New York: Spon Press, 2003.